

PAPER • OPEN ACCESS

Determination of compressive strength of 3D polymeric lattice structure as template in powder metallurgy

To cite this article: M S Utomo *et al* 2019 *IOP Conf. Ser.: Mater. Sci. Eng.* **541** 012042

View the [article online](#) for updates and enhancements.

Determination of compressive strength of 3D polymeric lattice structure as template in powder metallurgy

M S Utomo¹, Y Whulanza^{2,3}, F P Lestari¹, A Erryani¹, I Kartika¹ and N A Alief³

¹Research Center for Metallurgy and Materials – Indonesian Institute of Sciences, Indonesia

²Research Center for Biomedical Engineering – Universitas Indonesia, Indonesia

³Department of Mechanical Engineering – Universitas Indonesia, Indonesia

E-mail: muha209@lipi.go.id

Abstract. Powder metallurgy has been developed to fabricate metal foams from various materials including magnesium. One particular challenge on powder metallurgy is fabrication of highly-ordered and interconnected porous products. Pores interconnectivity is important in application of porous magnesium alloy for biodegradable orthopedic implants. Meanwhile, 3D polymeric printing technology offers capability to build precise and rapid lattice wireframe products in a simple and low-cost manner. Here, we design and validate the capability of 3D polymeric lattice as template in powder metallurgy for fabrication of magnesium-based biodegradable implants. Lattice structures were made of ABS, PLA, and PVA filaments. Lattice structures were cubical-shaped with uniform dimension and variations in pore size are included in the study. Both computational and experimental tests are performed to determine the compressive strength of the lattice structures. Uniaxial stress with uniform magnitude is applied to test the lattice structures. The resulting stress, strain, and deformation of the 3D polymeric lattice are observed. Variations in materials and pore size affect the stress, strain and deformation of the 3D polymeric lattice. Parameters can be further optimized to meet the requirement of the design and fabrication process in consideration of the tolerable stress, strain and deformation.

1. Introduction

The need for orthopedic implants is increasing over time. Degenerative diseases such as osteoarthritis and osteoporosis among growing population have driven the growth of the orthopedic implant market in global. In addition, accidental cases such as work accidents, traffic accidents, and sports injuries have been the cause of the increasing demand for orthopedic implants [1].

To fulfill its function to replace bone tissue, implants have certain criteria that must be met through the selection of materials and appropriate fabrication techniques. Based on their use, implants are divided into two categories: hard tissue / bone replacement implants such as fracture plates, screws, pins, and dental implants; and soft tissue replacement implants such as vascular implants [2].

The advantage of metal-based orthopedic implants compared to non-metals is that mechanical properties are better and more suitable for their function [3]. However, metal-based implants have a disadvantage when the implant must be planted for a long time in the patient's body. This can increase the risk of complications due to implant toxicity caused by the accumulation of metal ions formed from the corrosion process. Another disadvantage is different mechanical parameters with bone.

The difference in Young's modulus between implants and bone can make loss of bone tissue due to the shielding stress phenomenon. This phenomenon occurs because of the accumulation of load on the implant that reduces the burden on the bone in accordance with Wolff's law which states that the



formation of human bones will adjust to the supported load, if the load received by the bone decreases then the bone density will decrease and weaken because there is no stimulus to maintain bone mass [4].

Biodegradable implants are an alternative to permanent implants as implants that are temporary and able to decay within a period of time after bone tissue grows so that implant removal surgery is not required anymore from the patient's body. Metallic implants can be developed from titanium or magnesium materials which have mechanical properties, biocompatibility, and overall compatibility for the human body [5].

In designing a biodegradable implant, there is one important factor that must be considered, namely its ability to become scaffold or to grow and develop new bone tissue. Hopefully, the implant is capable of having a balanced overall rate of growth of new bone tissue so that when the implant decays perfectly, the bone tissue is mature enough and able to function like normal adult bone tissue. To be able to meet this criterion, the implant should have pores with certain dimensions that are connected to each other as a place to grow new bone tissue. Studies show that osteointegration processes occur best at pore sizes of 100-700 microns and porosity level at 60-80%. Interconnected pores facilitate fluid flow that gives cells to proliferate inside the implant and fully integrate with metal implants [6].

The porosity level is defined as the ratio between the volume of the pore cavity to the volume of implants which affects the mass and mechanical properties of implants such as Young's modulus, tensile strength, and compressive strength. Increasing the porosity level affects the mechanical strength of implants and implants with the same degree of porosity and different pore sizes have different mechanical properties. By modifying the porosity level, metal-based implants can be designed to have mechanical properties similar to human bones.

The process of making implants with complex internal architecture such as interconnected pores can be done, among others, through three-dimensional printing techniques. Three-dimensional printing techniques for metal materials are carried out through a pattern sintering process such as SLS (selective laser sintering), SLM (selective laser melting), or EBM (electron beam melting) [7]. SLS and SLM use lasers while EBM uses electron shots [8]. However, these processes require relatively expensive tools so that the cost of producing a complete implant cannot be reduced. Moreover, these processes also do not allow the manufacture of complete implants with magnesium-based materials because of their reactive properties so that the commonly used fabrication techniques are powder metallurgy with compacting and sintering.

Meanwhile, 3D polymeric printing technology offers capability to build precise and rapid lattice wireframe products in a simple and low-cost manner. Here, we numerically study the capability of 3D polymeric lattice as template in powder metallurgy for fabrication of magnesium-based biodegradable implants.

2. Materials and Methods

3D models of polymeric lattices are built on SolidWorks 2013. The models are then converted and transferred into Comsol Multiphysics 5.3 for numerical simulation of compressive stress test. Cubical shape is chosen to represent basic shapes of lattice structures. The lattices dimension are 15 mm x 15 mm x 15 mm. Although, to reduce simulation load, the dimension of the tested lattices are reduced into 5 mm x 5 mm x 15 mm. To compensate this reduction, the applied compressive load is proportionally adjusted. During compression process of powder metallurgy, the polymeric lattice structure will be subjected to uniaxial 300 psi compressive load. Two lattice pore sizes are used which are 1000 and 1500 microns. They refer to the requirement for the bone tissue growth and possibility of shrinkage during the fabrication process. The shape of the lattice is square. The wire of the lattice is approximately 200 microns in diameter. The wire diameter of the lattice is obtained based on the default nozzle size of the 3D polymer printer.

Three materials are used as the polymeric lattice materials which are acetyl butyl styrene (ABS), poly lactic acid (PLA), and poly vinyl alcohol (PVA). These materials are selected since all of them are common materials to be used as filaments in polymeric 3D printer. The mechanical properties of each materials are presented in Table 1. Another aspect on the material selection beside mechanical properties

and practicality is the biocompatibility and biodegradability properties. PLA is known for its biocompatibility and biodegradability. PLA itself has been developed as polymer-based implant. All selected materials are soluble in water-based solvent such as ethanol, chloroform, and DMO, each with their own dissolution rates.

Table 1. Mechanical properties of ABS, PLA, and PVA

Parameters	ABS	PLA	PVA
Density (kg/m ³)	1010 - 1200	1250	1120
Ultimate tensile strength (MPa)	33 - 110	35	32 - 66.2
Young's Modulus (GPa)	1.1 – 2.9	3.5	1.0 - 2.2
Poisson's ratio	0.35	0.36	0.45

3. Results and Discussion

Finite element analysis was performed using Comsol. Beforehand, 3D model of polymeric lattices was built using Solidworks. The 3D model was converted into STL format and imported as 3D component domain. Materials for the model were ABS, PLA, and PVA. Structural mechanics was applied as the governing physics for the environment. Two surface boundary conditions were defined: load and fixed constraints. The actual uniaxial compression was represented as loads located on top of the model and directed downward along y-axis. The applied load is 300 psi which represent the actual compression load. Fixed constraints were located at the bottom of the model. Discretization was then performed on the 3D model. The discretization generated 35000 cells and 40000 nodes. The calculation steps were formulated and the computational analysis was executed. Mesh convergence is performed to validate the numerical calculation result and discussed separately. Distribution of von Mises stress, strain, and displacement were selected as the output parameters visualized by color scales and minimum-maximum values. Figure 1 shows the 3D visualization of the proposed polymeric lattice designs. There are two designs, two cubical-based geometries with 1000X1000X1000 and 1500X1500X1500 cu.µm open pores. Designs with basic geometrical shapes are proposed as references to more complex designs in the future. Figure 2 shows the discretization result of the 3D model of the polymeric lattice. Figure 3 shows the distribution of von Mises stress on the 3D model of the polymeric lattice made from ABS under uniaxial compressive load of 300 psi. Figure 4 shows the distribution of strain on the 3D model of the polymeric lattice made from ABS under uniaxial compressive load of 300 psi. Figure 5 shows the distribution of displacement on the 3D model of the polymeric lattice made from ABS under uniaxial compressive load of 300 psi. Figure 6 shows graphs comparing the maximum von Mises stress for all variants. Moreover Figure 7 shows graphs comparing the displacement for all variants.

Computational simulation results show that the polymeric lattice structure is deformed mainly in the middle layer. It means that the middle layer is the weakest part of current lattice structure. It suggests that when the lattice structure is compressed during fabrication of porous magnesium alloy, the middle layer will have highest potential to be deformed. This becomes important for the fabrication of porous magnesium alloy due to potential of arising non-uniformity. Non-uniformity at the porous magnesium alloy might arises from two mechanisms. First mechanism is that the compressed and deformed middle layer compacts the powder around the area. This issue might produce a solid non-porous middle layer in the porous magnesium alloy. The other mechanism is that the compressed and deformed middle layer inhibits powder to infiltrate into the gaps. This might produce a cavity in the middle layer of the porous magnesium alloy. The prediction of stress is not as accurate as prediction of displacement due to stress assumption over the object. In addition, factors such as element/mesh size, might affect the accuracy of the output value [15].

Effect of lattice shape to compressive properties on 3D-printed ABS material has been carried out. Honeycomb-like cellular lattice structure has the highest mechanical properties among other shapes such

as rectangular, triangular, and circular. Although, the difference was not significant. Meanwhile, increase in porosity also decrease mechanical strength [14]. PLA has also been observed to exhibit shape-memory effect which can be triggered by thermal stimuli [17]. The 3D printing fabrication technique also introduce internal stress/strain to the polymer material due to the heating/cooling process. There are several ways to improve the mechanical properties of 3D-printed product, either by modifying the process or the material. Material modification can be performed through addition of fibers or particles made from glass, carbon, or polymers. Such treatment can improve the tensile strength of 3D-printed product up to 50% [16].

Foams material and lattice structures have fundamental difference. Foams material has a solid structure filled with cavities with varying size and shape. It can form closed cell or open cell foam material. Meanwhile, lattice structures are assembled by identical skeletal structure forming three dimensional geometrical shapes such as cubes or cylinders. Pores are shaped due to the spatial between skeletal structures. There are several types of lattice structures such as Kagome, hexagonal diamond, and cross pyramidal. Each lattice structures has its own mechanical behavior to withstand compressive stress which can be observed through the stress-strain curve [9].

Fabrication of metallic lattices using additive manufacturing by selective laser melting analyzed by numerical and experimental compressive tests has been conducted [10,11,12]. Theoretical approach to determine mechanical behavior of lattice structures under compressive loading has been proposed [13]. The lattice are subjected to compression or tension load and bending without twisting moment when subjected to uniaxial compressive loading, which according to Euler-Bernoulli beam theory is linearly distributed over the cross section.

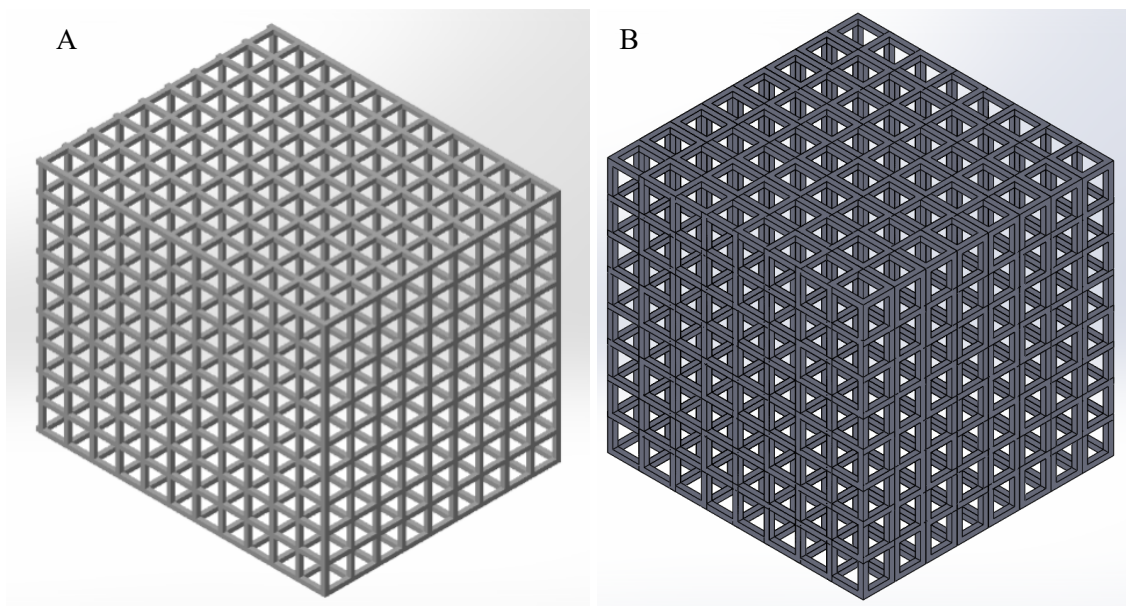


Figure 1. 3D visualization of cubical lattice structure with 1000X1000X1000 (A) and 1500X1500X1500 (B) cu.µm open pore volume.

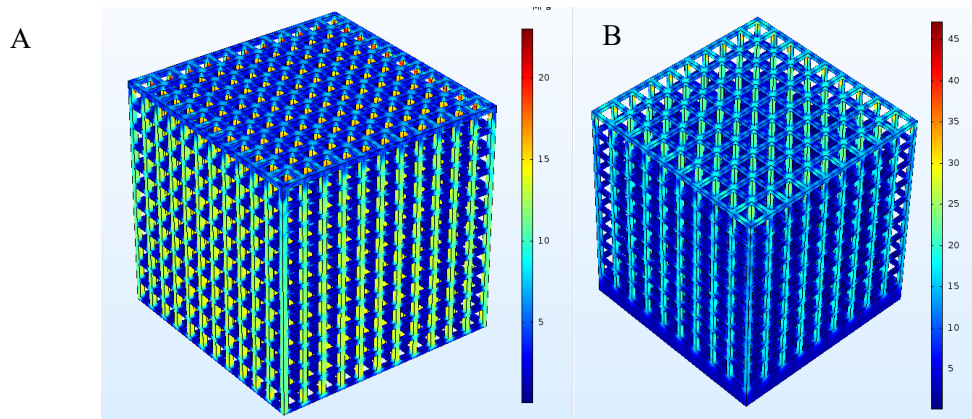


Figure 2. Visualization of von Mises stress distribution on ABS material, 1000X1000X1000 (A) and 1500X1500X1500 (B) cu.µm open pore volume.

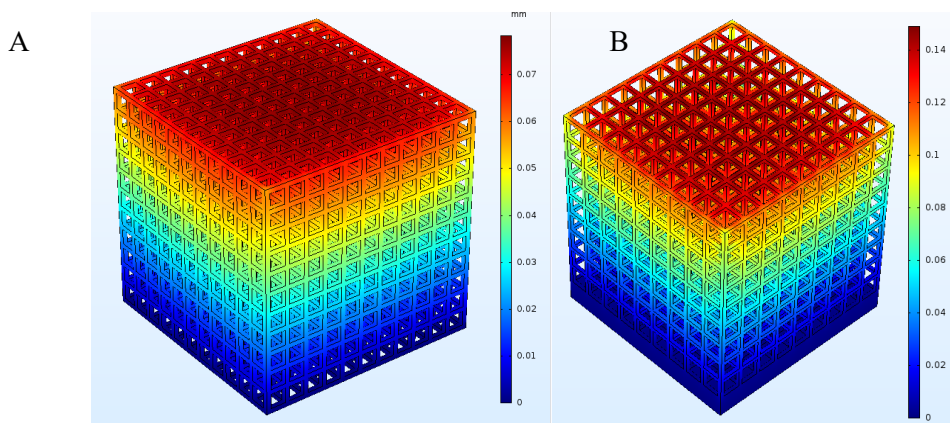


Figure 3. Visualization of displacement distribution on ABS material, 1000X1000X1000 (A) and 1500X1500X1500 (B) cu.µm open pore volume.

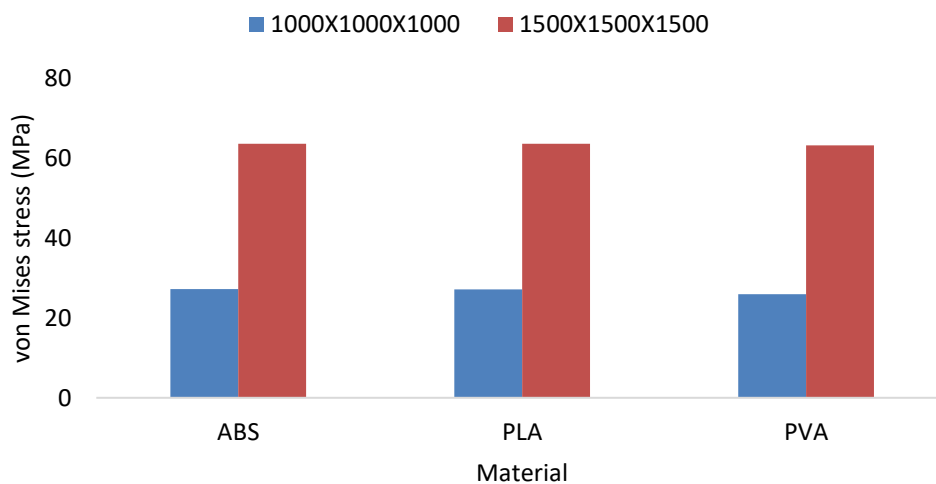


Figure 4. Graph comparing maximum von Mises stress distribution shows material variation does not affect the amount of stress acting on the structure while reduction of pore size from 1500X1500X1500 to 1000X1000X1000 cu.µm reduces the maximum value of von Mises stress to half.

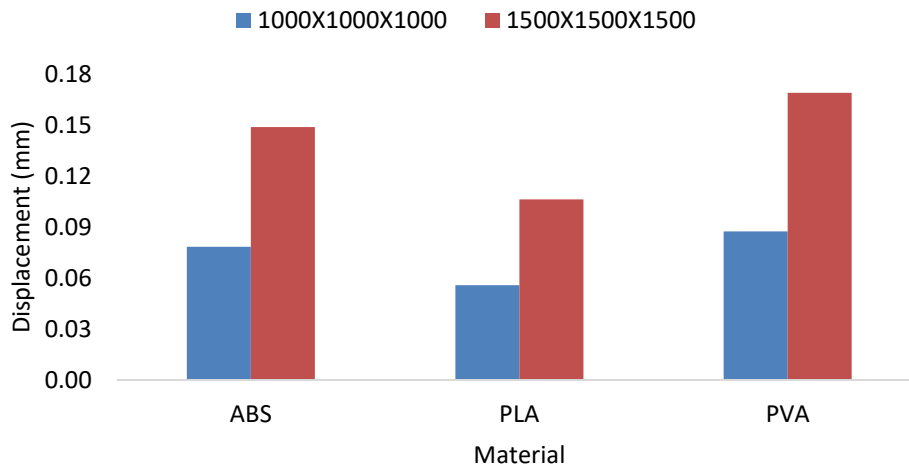


Figure 5. Graph comparing maximum displacement shows both material and pore size variation affect the maximum displacement value. PLA shows lowest value of deformation on both pore sizes. while PVA shows highest value of deformation on both pore sizes.

4. Conclusion

Design and numerical validation of 3D polymeric lattice has been presented. Three commercially-available filament materials (ABS, PLA, and PVA) are used to fabricate lattice structures with variation in shape and pore size. Each structure is subjected to uniform uniaxial compressive load. Difference in material and geometry made each lattice structures distribute compressive stress load in different ways leading to different deformation pattern. Under same outer dimension and uniform pore distribution, different pore size alters the porosity/pore density.

References

- [1] R Magetsari, Suyitno, R Dharmastiti, UA Salim, L Hidayat, T Yudiman, Z A Lanodiyu, dan P Dewo, *International Journal of Morphology* **33**(4), 2015, pp. 1255-1260.
- [2] C J Pendegrass, *Doctoral thesis, University of London*, 2005.
- [3] S Toghiani dan M Khodaei, *Materials Research Express* **5**, 2018.
- [4] S W Kim, H D Jung, M H Kang, H E Kim, Y H Koh, Y Estrin, *Materials Science and Engineering C* **33**, 2013, pp. 2808-2815.
- [5] M K Datta, D T Chou, D Hong, P Saha, S J Chung, B Lee, A Sirinterlicki, M Ramanathan, A Roy, dan P N Kumta, *Materials Science and Engineering B* **176**, 2011, pp. 1637-1643.
- [6] S Dutta, K B Devi, dan M Roy, *Advanced Powder Technology*, 2017.
- [7] G Jiang, Q Li, C Wang, J Dong, dan G He, *Materials and Design*, 2014.
- [8] I Maskery, N T Aboulkhair, A O Aremu, C J Tuck, I A Ashcroft, R D Wildman, dan R J M Hague, *Materials Science and Engineering: A*, volume **670**, 2016, pp. 264-274.
- [9] S K Moon, Y E Tan, J Hwang, and Y J Yoon, *International Journal of Precision Engineering and Manufacturing-Green Technology* vol. **1** No. 3, pp. 223-228 (2014).
- [10] R Mahshid, H N Hansen, and K Loft-Hojbjerre, *Materials & Design* **104**, pp. 276-283 (2016).
- [11] D Noviello, *Autodesk University*, pp. 1-22.
- [12] O Rehme and C Emmelmann, *Proc. of SPIE* Vol. **6107**, pp. 1-12 (2006).
- [13] K Ushijima, W J Cantwell, and D H Chen, *Journal of Computational Science and Technology* vol. **4** No. 3, pp. 159-171 (2010).
- [14] O Iyibilgin, C Yigit, and M C Leu 2013 *Proceedings of Solid Freeform Fabrication Symposium*, 895-907
- [15] Dutt A 2015 *Int. Jour. of Eng. Sci. and Innovative Technology* **4**(3) 181-185

[16] Wang J, Xie H, Weng Z, Senthil T, and Wu L 2016 *Materials and Design* **105**, 152-159

[17] Zhang Q, Yan D, Zhang K, and Hu G 2015 *Scientific Reports* **5** 1-6

Acknowledgement

This research is funded by Insinas grant scheme from Ministry of Research and Higher Education.